Settlements and pore pressure generation in sand during earthquakes - physical phenomena and their 1-D description

A. Niemunis, T. Wichtmann, Th. Triantafyllidis

Institute of Soil Mechanics and Foundation Engineering, Ruhr-University Bochum, Germany

Abstract

This paper discusses the pore water pressure generation due to earthquake shaking. Moreover a method of settlement prediction during the reconsolidation phase is presented. The cumulative effects are calculated with an explicit (N-type) constitutive model.

Keywords: liquefaction, earthquake, non-linear wave, explicit accumulation model, dissipation

1 Introduction and notation

Even in a simple 1-D case the liquefaction of a sand layer, Fig. 1, due to an earthquake is a relatively complex phenomenon. The sand layer of the thickness H is harmonically excited in the horizontal direction at the rock bed level ($x = 0$). In the horizontal direction the phenomena are homogeneous over a large area. This allows for a 1-D approach. The excitation at the rock bed causes a shear wave that propagates vertically upwards, possibly with a reflection at the top ($x = H$). The propagation of the shear wave with an energy dissipation $D(\gamma^{\text{ampl}}, \boldsymbol{\sigma}')$ and with a nonlinear shear modulus $G(\gamma^{\text{ampl}}, \boldsymbol{\sigma}')$ is not a straightforward problem. Additionally a considerable accumulation of strain $\dot{\boldsymbol{\epsilon}}^{\text{acc}}$ and of cyclic relaxation $\dot{\boldsymbol{\sigma}}'^{\text{acc}}$ appears as a side effect. This is accompanied by the generation of excess pore water pressure and its subsequent dissipation.

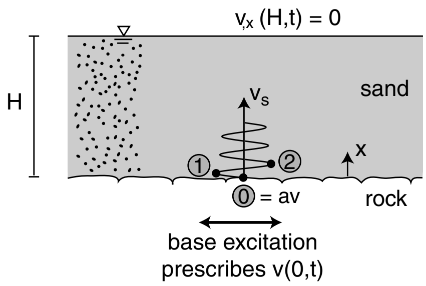

Figure 1: *Shear wave that propagates vertically in a saturated sand layer*

The phenomena mentioned above are interrelated. For example, the shear stiffness G and the damping ratio D depend on the shear strain amplitude γ^{ampl} (which requires a rate type description $\dot{\tau} = G\dot{\gamma}$) and on the mean effective stress p, which makes the amplitude dependent of the accumulated pore pressure. In the opposite direction, the size of the amplitude influences strongly the rate of cyclic relaxation (or pore pressure build-up) which eventually leads to a feed-back effect. The rate $u_{,t}$ of the dissipation of the generated excess pore pressure u is related to the second spatial derivative $u_{,xx}$ as known from the Terzaghi's consolidation theory. Moreover this rate depends on u because the coefficient of consolidation $c_v = kE/(g\rho_w)$ contains the stiffness modulus E which depends on the effective mean pressure (i.e. indirectly on u).

In our opinion an investigation of the pore pressure generation independently of the dynamic analysis, e.g. assuming an empirical distribution of the shear amplitude, e.g. [4], is oversimplified. As shown by the Karlsruhe soil mechanics group, e.g. [2], a liquefied zone separates the layers above reflecting (at least partly) the shear wave. Obviously this separation causes a redistribution of the amplitudes along the depth.

From the point of view of numerical simulations the consideration of complicated cumulative phenomena and pore pressure dissipation together with already for itself strongly nonlinear and dissipative equations of soil dynamics seems difficult. Therefore, in this paper we propose a mixed numerical strategy based on the explicit accumulation model recently developed in Bochum [3, 6]. An important simplification we make is to decouple the dynamic and quasi static phenomena. The idea is to fix several slowly changing variables for a period T of a single excitation. These variables are updated after a full cycle only. The quick variables (appearing in the dynamic equations) are calculated using time increments much smaller than the period T. This strategy can be presented with the following flowchart:

1. Initialize all fields with the basic state variables of the problem. By convention, if a field has two arguments the first one denotes the position x and the second is time t (or the number of cycles $N = t/T$ if the slow variable changes stepwise). The fields of state variables can be grouped into two lists: continuous and stepwise (in time). For $t = 0$ and $N = 0$ we have to prescribe the following initial conditions (IC):

   - time-continuous variables:
     $v(x, t), \tau(x, t), \gamma(x, t), \dot{\gamma}(x, t)$
   - stepwise variables:
     $e^{\text{av}}(x, N), \boldsymbol{\sigma}'^{\text{av}}(x, N), u^{\text{av}}(x, N), v^{\text{ampl}}(x, N), \gamma^{\text{ampl}}(x, N)$

   All of these variables are usually initialized with zeros except for the stress $\boldsymbol{\sigma}'^{\text{av}}(x, N) = -\rho g(H - x)\{1, K_0\}$ and the void ratio $e^{\text{av}}(x, N)$.

2. Calculate a single period of excitation of the rock bed from t to $t + T$. For this calculation we assume the boundary conditions (BC) given by: $v(0, t) = v_0^{\text{ampl}} \sin(2\pi t/T)$ and $v_{,x}(H, t) = 0$ (stress free surface). The discrete variables, in particular the average effective stress $\boldsymbol{\sigma}'^{\text{av}}$ and the void ratio e^{av} remain constant during this calculation. We have to memorize the reversal points of the the strain and stress paths to estimate their amplitudes. For details see Section 2.1. After the dynamic calculation the time t is increased by T. Also the discrete time variable N (= the cycle number) should be increased by 1.

3. Calculate the amplitudes $\gamma^{\text{ampl}}(x, N)$ and $\tau^{\text{ampl}}(x, N)$ from the two recently recorded reversal values of the paths $\gamma(x, t)$ and $\tau(x, t)$. These amplitudes enter the explicit formula for the increment of irreversible strain $\dot{\boldsymbol{\epsilon}}^{\text{acc}} = \mathbf{m} f(\ldots)$. Using this increment we update the effective stress $\boldsymbol{\sigma}'^{\text{av}}(x, N)$, the void ratio $e^{\text{av}}(x, N)$ and the pore pressure $u^{\text{av}}(x, N)$ as described in Section 2.2.

4. Finally we calculate the dissipation of pore pressure that occurs during the period T. The corresponding vertical deformation leads to settlements and to the densification of the sand, see Section 2.3.

5. After all time-discrete variables are updated we should control the applicability of the constitutive model $\dot{\tau} = \dot{\tau}(\sigma'_v, \tau, \dot{\gamma})$ because one of two equations can be used: one for hysteretic cycles and one for the cyclic mobility cycles (stress path encounters the yield criterion). Note that the void ratio e influences the critical stress p_{crit}.

6. Return to the point 2 of this flowchart and continue.

1.1 Notation

The vertical coordinate x is directed upwards with $x = 0$ at the rock bed, see Fig. 1. Stress and (small) strain are used with the mechanical sign convention (tension positive). The superscripts $\sqcup^{\text{ampl}}$, $\sqcup^{\text{av}}$ and $\sqcup^{\text{acc}}$ denote the amplitude, the average and the accumulated values, respectively. The superposed dot $\dot{\sqcup}$ denotes the rate i.e. the derivative with respect to the second argument (which can be either N or t). The subscripts $\sqcup_v$ and $\sqcup_h$ refer to the vertical and the horizontal direction. The subscripts with a variable following comma, e.g. $\sqcup_{,t}$ or $\sqcup_{,xx}$ denote differentiation with respect to this variable. The normalization operator denoted as $\vec{\sqcup} = \sqcup / \| \sqcup \|$ should be understood tensorially, i.e. if $\sqcup$ is a 2:1 matrix, the full 3:3 tensor should be recovered, normalized and the respective components should be extracted from the result and put back to the 2:1 form.

Below, all primary state variables are listed:

1. horizontal velocity $v(x,t)$ with $v_{,x}(x,t) = \dot{\gamma}(x,t)$
2. shear stress $\tau(x,t)$
3. strain $\boldsymbol{\epsilon}(x,N) = \{\epsilon_v, \epsilon_h\}^T$
4. effective stress $\boldsymbol{\sigma}'(x,N) = \{\sigma'_v, \sigma'_h\}^T$. The total stress is $\boldsymbol{\sigma}$. The Roscoe invariants are $p = -\frac{1}{3}(\sigma'_v + 2\sigma'_h)$ and $q = -(\sigma'_v - \sigma'_h)$.
5. excess pore pressure $u(x,N)$

Some of the derived state variables are:

1. shear strain $\gamma(x,t)$ obtained by integration of $\dot{\gamma}(x,t)$
2. amplitude of shear strain $\gamma^{\text{ampl}}(x,N)$ and shear stress $\tau^{\text{ampl}}(x,N)$
3. elastic normal stiffness $\mathsf{E}(x,N)$ and shear stiffness $G(x,t)$
4. strain accumulation rate $\dot{\boldsymbol{\epsilon}}^{\text{acc}}(x,N)$
5. consolidation coefficient $c_v(x,N)$
6. yield stress $\sigma'_Y(x,N)$

2 Physical phenomena to be considered

2.1 Plasto-dynamic shear wave

The plasto-dynamic shear wave (with density ρ and not ρ_d or ρ') must consider the nonlinear stiffness which changes with the stress τ and with the direction of strain rate $\dot{\gamma}$. Moreover, the stiffness depends on the effective normal stress $\boldsymbol{\sigma}'$ which varies with the pore pressure on one hand and with the depth $(H-x)$, Fig. 1, on the other hand. The wave equations

$$\begin{aligned} \rho v_{,t} - \tau_{,x} &= 0 \qquad (1)\\ G v_{,x} - \tau_{,t} &= 0 \qquad (2) \end{aligned}$$

consider the conservation of momentum and the constitutive equation with the nonlinear shear modulus $G = G(v_{,x}, \tau)$. Assuming the shear wave with horizontal polarization no vertical mass transport and no advective terms need to be considered. Changes of density ρ within a single period are also neglected. For the dynamic calculations we distinguish two kinds of shear response:

- The hysteretic behaviour, Fig. 2a, is described by $\dot{\tau} = G_L(\dot{\gamma} - \frac{\tau}{\tau_Y}|\dot{\gamma}|)$, wherein $G_L = G_L(\boldsymbol{\sigma}'^{\text{av}})$ is the linear term and τ_Y is the yield stress which is calculated from the condition that the superposition of $\boldsymbol{\sigma}'^{\text{av}}$ with τ_Y satisfies the Coulomb criterion

  $$\frac{\frac{1}{4}(\sigma'_v - \sigma'_h)^2 + \tau_Y^2}{\frac{1}{4}(\sigma'_v + \sigma'_h)^2} = \sin^2\varphi \qquad (3)$$

  As we discuss in Section 2.2 after several cycles an isotropic average stress establishes itself. In this case the superposition of shearing leads to $|\tau_Y/\sigma'| = \sin\varphi$ (and not $\tan\varphi$).

- Unless the sand is extremely loose (no rapid collapse) cyclic mobility is observed, Figs. 2b and 3. This is described by $\dot{\tau} = G\dot{\gamma}$ in which $G = G_r + |c_1\tau - (\tau_0 + c_2|\tau|)\text{sign}(\dot{\gamma})|$. The small residual stiffness G_r is related to the viscosity of the sand at vanishing effective stress. This description should be supplemented by the condition $|\tau| < \sigma_{\text{crit}}\sin\varphi$, wherein $\sigma_{\text{crit}}(e)$ corresponds to the critical state.

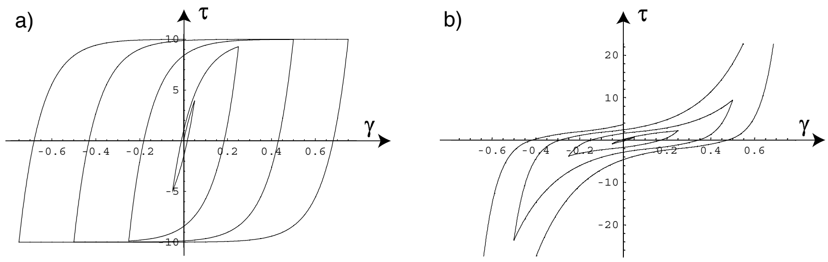

Figure 2: *1-D γ-τ-cycles generated numerically with $\dot\tau = G\dot\gamma$ wherein a) $G = G_L(1 - \operatorname{sign}(\dot\gamma)\tau/\tau_Y)$ and b) $G = |c_1\tau - (\tau_0 + c_2|\tau|)\operatorname{sign}(\dot\gamma)| + G_r$*

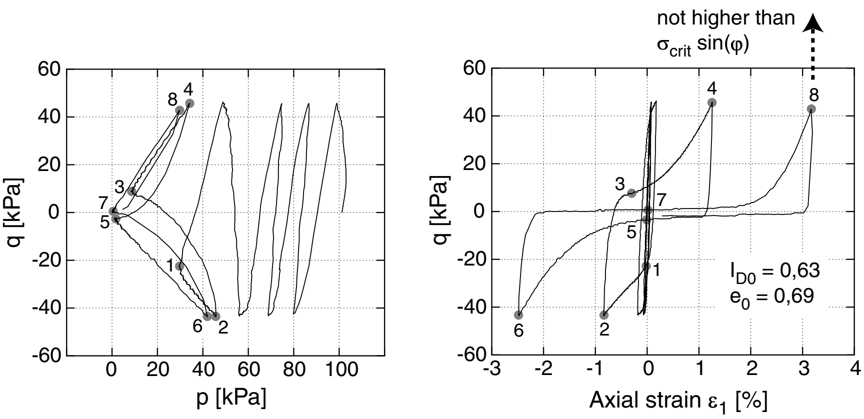

Figure 3: *Cyclic mobility in a stress-controlled cyclic triaxial test: a) effective stress path in the p-q-plane, b) stress-strain hysteresis*

2.2 Evolution of stress during pore pressure build-up

Under undrained conditions (assumed within the full cycle) the accumulation of strain causes an evolution of the effective stress according to

$$\dot{\boldsymbol{\sigma}}' = \mathsf{E} \cdot (\dot{\boldsymbol{\epsilon}} - \dot{\boldsymbol{\epsilon}}^{\mathrm{acc}} - \dot{\boldsymbol{\epsilon}}^{\mathrm{pl}}) \qquad \text{with} \qquad \operatorname{tr} \dot{\boldsymbol{\epsilon}} = 0 \tag{4}$$

wherein E is the elastic stiffness. This stiffness is pressure dependent and anisotropic, cf. [1]. Under the simplified conditions and for the K_0-stress state we have a transversally isotropic stiffness

$$\left\{ \begin{array}{c} \dot\sigma'_v \\ \dot\sigma'_h \end{array} \right\} = \lambda \left[\begin{array}{cc} E_v(1-\nu_{hh}) & 2E_v\nu_{hv} \\ E_h\nu_{vh} & E_h \end{array} \right] \cdot \left\{ \begin{array}{c} \dot\epsilon_v - \dot\epsilon_v^{\mathrm{acc}} - \dot\epsilon_v^{\mathrm{pl}} \\ \dot\epsilon_h - \dot\epsilon_h^{\mathrm{acc}} - \dot\epsilon_h^{\mathrm{pl}} \end{array} \right\} \tag{5}$$

with ν_{ij} being the anisotropic Poisson's ratios and $\lambda = 1/(1 - \nu_{hh} - 2\nu_{hv}\nu_{vh})$. For the numerical examples we have used $\nu_{hh} = 0.06, \nu_{hv} = 0.2, \nu_{vh} = 0.35$ and $E_v = 354(p/p_{\mathrm{atm}})^{0.5}$ MPa and $E_h = 198(p/p_{\mathrm{atm}})^{0.5}$ MPa for $e = 0.668$ and $K_0 = 0.45$ after [1].

In our 1-D problem we assume homogeneity in the horizontal direction and therefore $\dot\epsilon_h = 0$. Moreover, within a single cycle the undrained conditions are perfectly satisfied, $\dot\epsilon_v + 2\dot\epsilon_h = 0$, so also $\dot\epsilon_v$ must vanish. The components of accumulative strain $\dot{\boldsymbol{\epsilon}}^{\mathrm{acc}}$ are not identical because the inelastic accumulation has also a deviatoric part. The generation of pore pressure must be identical for both directions. The excess pore pressure can be found from the vertical stress component

$$\dot u = -\dot\sigma'_v \tag{6}$$

because the vertical component $\sigma_v = \sigma'_v + u = \rho g(H - x)$ of the total stress remains constant. This is not true for the horizontal component of the total stress which evolves due to (5) and due to the pore pressure build-up, viz. $\dot\sigma_h = \dot\sigma'_h + \dot u$.

The accumulation of strain can be expressed as

$$\dot{\boldsymbol{\epsilon}}^{\mathrm{acc}} = \mathbf{m} f(\ldots) \tag{7}$$

wherein $f(\ldots)$ consists of several functions, see [3, 6] or Fig. 4b, and

$$\mathbf{m} = \left\{ \begin{array}{c} m_v \\ m_h \end{array} \right\} = -\left\{ \begin{array}{c} 9 + M^2 + 4K(9+M^2) + K^2(-45+4M^2) \\ 18 + M^2 + K(9+4M^2) + K^2(9+4M^2) \end{array} \right\}^{\rightarrow} \tag{8}$$

with $K = \sigma_h'/\sigma_v'$ and $M = 6\sin\varphi/(3-\sin\varphi)$. The direction of flow $\mathbf{m}$ is a unit tensor found experimentally [6], Fig. 4a.

a)

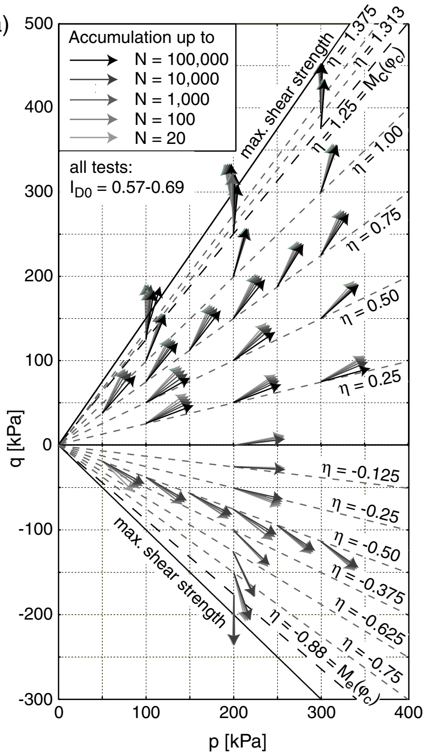

b)

Function	Mat. const./ Ref. value	
$f_{\mathrm{ampl}} = (\varepsilon^{\mathrm{ampl}} / \varepsilon^{\mathrm{ampl}}_{\mathrm{ref}})^2$	$\varepsilon^{\mathrm{ampl}}_{\mathrm{ref}}$	10^{-4}
$f_N^A = C_{N1}\, C_{N2} \exp(-g^A/C_{N1}/f_{\mathrm{ampl}})$	C_{N1}	$3.4 \cdot 10^{-4}$
$f_N^B = C_{N1}\, C_{N3}$	C_{N2}	0.55
	C_{N3}	$6.0 \cdot 10^{-5}$
$f_p = \exp[-C_p(p^{\mathrm{av}}/p_{\mathrm{ref}}-1)]$	C_p	0.43
	p_{ref}	100 kPa
$f_Y = \exp(C_Y\, \bar{Y}^{\mathrm{av}})$	C_Y	2.0
$f_e = \dfrac{(C_e - e)^2}{1+e} \dfrac{1+e_{\mathrm{ref}}}{(C_e - e_{\mathrm{ref}})^2}$	C_e	0.54
	e_{ref}	0.874
f_π = 1 if polarization = constant, else see [6]		

Figure 4: *a)Cyclic flow rule* $\mathbf{m}$ *shown as unit vectors in the* p-q*-plane, inclined with* $\varepsilon_q^{\mathrm{acc}}/\varepsilon_{\mathrm{vol}}^{\mathrm{acc}}$ *towards the* p*-axis, b) Function* $f(\ldots) = f_{\mathrm{ampl}}(f_N^A + f_N^B) f_p f_Y f_e f_\pi$ *depends on several factors, among others on the stress ratio* (f_Y) *and on the structural effects* (f_N^A)*. The material constants were evaluated for a medium coarse sand*

Let us begin with the K_0 stress $\boldsymbol{\sigma}'^{\mathrm{av}} = \{-158, -71\}^T$ (i.e. $p = 100$ kPa and $q = 87$ kPa) superposed by a shear stress τ^{ampl} small enough to keep the resulting Mohr circle within the elastic domain, Fig. 5. The plastic strains are absent and (8) gives $\mathbf{m} = \{-0.921, 0.275\}^T$. The pseudo relaxation

$$\dot{\boldsymbol{\sigma}}' = f(\ldots)\ \{334.4, 11.7\}^T \tag{9}$$

makes the stress more isotropic, Fig. 6. The stiffness E and G, the flow direction $\mathbf{m}$ and the flow intensity $f(\ldots)$ in (5) evolve with the changing effective stress.

If the condition (3) is satisfied either a butterfly-like p-q stress path (cyclic mobility) or (for extremely loose sands, i.e. $p > p_{\mathrm{crit}}(e)$ which we do not discuss here) a rapid collapse is observed. In both cases, however, the pore pressure generation continues until the vertical effective stress vanishes, $\sigma_v' = 0$. For sands (cohesionless soils) this implies $\boldsymbol{\sigma}' = \mathbf{0}$. If $\dot{u} = 0$ and $\boldsymbol{\sigma}' = \mathbf{0}$ the undrained condition implies the constant water volume. The accumulation of strain *in the soil skeleton* may continue, cf. [5]. This phenomenon has been implemented into the explicit model (function $f(\ldots)$) assuming $\mathbf{m} = -\mathbf{1}/\sqrt{3}$. If the volumetric deformations of water and skeleton are different then the reconsolidation begins with squeezing out the excessive volume of water (the latent deformation of the skeleton becomes visible) and subsequently the excess pore pressure is dissipated.

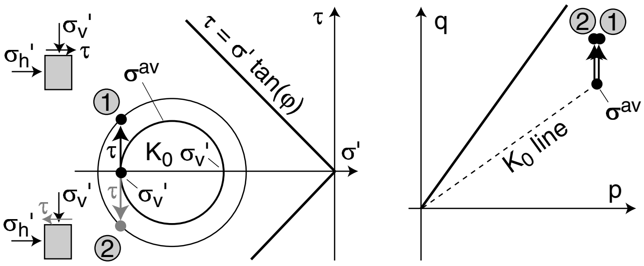

Figure 5: *State of stress within a stress cycle*

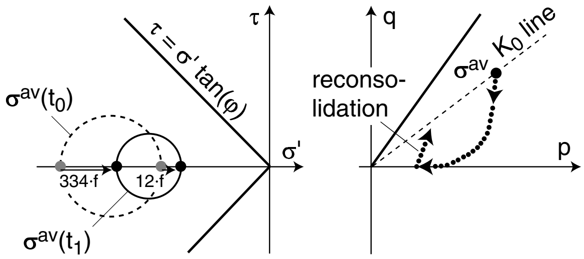

Figure 6: *Stress becomes more isotropic during pore pressure build-up*

2.3 Evolution of stress and strain during pore pressure dissipation

The consolidation and pore pressure redistribution starts from the initial $u(x, t_i) = u(x, N)$-field and lasts for a single period T only. The governing equation is

$$u_{,t} = c_v u_{,xx} \qquad \text{wherein} \;\; c_v = kE/(\rho_w g)\,. \tag{10}$$

Seepage forces are neglected. The ultimate result of the (partial) consolidation after each cycle is not only the pore pressure increment $\dot{u} = -\dot{\sigma}'_v$ but also the residual vertical strain increment $\dot{\epsilon}_v$ and the effective horizontal stress increment $\dot{\sigma}'_h$. They can be easily found from the equation system

$$\left\{ \begin{array}{c} -\dot{u} \\ \\ \dot{\sigma}'_h = ? \end{array} \right\} = \lambda \left[\begin{array}{cc} E_v(1-\nu_{hh}) & 2E_v\nu_{hv} \\ \\ E_h\nu_{vh} & E_h \end{array} \right] \cdot \left\{ \begin{array}{c} \dot{\epsilon}_v = ? \\ \\ 0 \end{array} \right\} \tag{11}$$

We have assumed that the reconsolidation is elastic and $\dot{\epsilon}_h = 0$. The solution is

$$\dot{\sigma}'_h = \frac{-E_h\nu_{vh}\dot{u}}{E_v(1-\nu_{hh})} \quad \text{and} \quad \dot{\epsilon}_v = \frac{-\dot{u}}{E_v\lambda(1-\nu_{hh})} \tag{12}$$

Comparing (9) with the ratio $\dot{\sigma}'_h/\dot{\sigma}'_v = 0.2$ obtained from (12) (for isotropic elasticity with $\nu = 0.2$ it would be 0.25) we conclude that the stress ratio $K = \sigma'_h/\sigma'_v$ increases if the accumulation and dissipation of pore pressure occur simultaneously and decreases if the dissipation follows the generation.

References

[1] R. Kuwano, T.M. Connolly, and R.J. Jardine. Anisotropic stiffness measurements in a stress-path triaxial cell. *Geotechnical Testing Journal, ASCE*, 23(2):141–157, 2000.

[2] I. Loukachev. Dilatanzwellen und Schichttrennung bei Wellenausbreitung in sandigen Böden. PhD thesis, Institut für Boden- und Felsmechanik der Universität Karlsruhe, Issue No. 155, 2002.

[3] A. Niemunis, T. Wichtmann, and T. Triantafyllidis. A high-cycle accumulation model for sand. *Computers and Geotechnics*, 32(4):245–263, 2005.

[4] H.B. Seed and I.M. Idriss. Simplified procedure for evaluating soil liquefaction potential. *Journal of the Soil Mechanics and Foundations Division, ASCE*, 97(SM9):1249–1273, 1971.

[5] Y. Shamoto, M. Sato, and J.-M. Zhang. Simplified estimation of earthquake-induced settlements in saturated sand deposits. *Soils and Foundations*, 36(1):39–50, 1996.

[6] T. Wichtmann, A. Niemunis, and T. Triantafyllidis. Strain accumulation in sand due to cyclic loading: drained triaxial tests. *Soil Dynamics and Earthquake Engineering*. (in print).